Talanta 122 (2014) 122–129

Contents lists available at ScienceDirect

Talanta

journal homepage: www.elsevier.com/locate/talanta

Kinetic performance comparison of fully and superficially porous particles with a particle size of 5 μm: Intrinsic evaluation and application to the impurity analysis of griseofulvin

Getu Kahsay [a], Ken Broeckhoven [b], Erwin Adams [a], Gert Desmet [b], Deirdre Cabooter [a,*]

[a] KU Leuven, Department of Pharmaceutical Sciences, Pharmaceutical Analysis, Herestraat 49, O&N 2, PB 923, 3000 Leuven, Belgium
[b] Vrije Universiteit Brussel, Department of Chemical Engineering, Pleinlaan 2, 1050 Brussels, Belgium

ARTICLE INFO

Article history:
Received 30 October 2013
Received in revised form
15 January 2014
Accepted 20 January 2014
Available online 31 January 2014

Keywords:
Kinetic plots
Superficially porous particles
Loadability
Griseofulvin
5 μm particles

ABSTRACT

After the great commercial success of sub-3 μm superficially porous particles, vendors are now also starting to commercialize 5 μm superficially porous particles, as an alternative to their fully porous counterparts which are routinely used in pharmaceutical analysis. In this study, the performance of 5 μm superficially porous particles was compared to that of fully porous 5 μm particles in terms of efficiency, separation performance and loadability on a conventional HPLC instrument. Van Deemter and kinetic plots were first used to evaluate the efficiency and performance of both particle types using alkylphenones as a test mixture. The van Deemter and kinetic plots showed that the superficially porous particles provide a superior kinetic performance compared to the fully porous particles over the entire relevant range of separation conditions, when both support types were evaluated at the same operating pressure. The same observations were made both for isocratic and gradient analysis. The superior performance was further demonstrated for the separation of a pharmaceutical compound (griseofulvin) and its impurities, where a gain in analysis time of around 2 could be obtained using the superficially porous particles. Finally, both particle types were evaluated in terms of loadability by plotting the resolution of the active pharmaceutical ingredient and its closest impurity as a function of the signal-to-noise ratio obtained for the smallest impurity. It was demonstrated that the superficially porous particles show better separation performance for griseofulvin and its impurities without significantly compromising sensitivity due to loadability issues in comparison with their fully porous counterparts. Moreover these columns can be used on conventional equipment without modifications to obtain a significant improvement in analysis time.

1. Introduction

Despite the impressive improvements made in separation efficiency and analysis time by the introduction of small particle columns operated at ultra-high pressures, pharmaceutical analyses are still largely performed on conventional, 250 × 4.6 mm fully porous 5 μm particle columns [1]. This certainly has to do with the fact that numerous official methods (cfr. Pharmacopoeia analyses) are described on these large particle columns and that many pharmaceutical laboratories simply are not yet equipped with the most recent, low-dispersion ultra-high performance liquid chromatographs (UHPLC).

As a compromise to obtain ultra-high efficiencies at conventional backpressures, superficially porous particles (also called core–shell particles) were (re-)introduced on the market in 2006. These particles, with a typical nominal diameter of 2.6–2.7 μm, consist of a solid core surrounded by a porous shell. It has been demonstrated on multiple occasions that superficially porous particles exhibit extra-ordinarily high efficiencies, with minimum reduced plate heights ranging between 1.3 and 1.5 [2–4].

The relatively large size of the core–shell particles (in comparison with sub-2 μm fully porous particles), moreover results in permeability values and hence column backpressures that are compatible with conventional HPLC instrumentation. In fact, it has been demonstrated that – due to the combination of high column efficiency and permeability – superficially porous particles are able to reach plate counts in the practical range of separation efficiencies equally fast as fully porous sub-2 μm particles, when the latter are operated at 1000 bar and the former only at 600 bar [5,6].

It has, however, been suggested that conventional LC systems are not suitable to record the peaks eluting from these high-efficiency core–shell columns. A conventional HPLC can easily contribute up to 50% of the peak variance for e.g. a core–shell column with dimensions of 50 × 4.6 mm, eluting a compound with

* Corresponding author. Tel.: +32 16323442; fax: +32 16323448.
E-mail address: deirdre.cabooter@pharm.kuleuven.be (D. Cabooter).

0039-9140/$ - see front matter © 2014 Elsevier B.V. All rights reserved.
http://dx.doi.org/10.1016/j.talanta.2014.01.050

a retention factor of $k=1$ [7], hence causing a significant loss of the true column efficiency. For narrower columns (2.1 mm I.D.) this system contribution increases even more, leading to unacceptable losses in performance. Gritti et al. [7] proposed to make some changes to a conventional HPLC to minimize its extra-column contributions. They reduced the extra-column volumes of the instrument and focused the analyte band on top of the column to reduce its width. In this way, they demonstrated an increase in column efficiency of 28%, 41% and 278% for core–shell columns with dimensions of 100 × 4.6 mm, 50 × 4.6 mm and 50 × 2.1 mm respectively, for a compound with $k=1.5$.

In order to reach high separation efficiencies without making modifications to the instrument, core–shell particles with particle sizes of 4.6–5.0 μm have recently been launched. These particles are structurally very similar to their sub-3 μm counterparts, with a core-to-particle diameter of around $\rho=0.73$, and represent a significant advantage in separation performance compared to both 3.5 μm and 5 μm fully porous particles. These high performances have been demonstrated on state-of-the-art UHPLC instrumentation [1,3,8], but should equally well be attainable on conventional HPLC equipment when packed in 250 × 4.6 mm I.D. columns, due to the large accessible volume of these columns (hold-up volume for a 250 × 4.6 mm column with a total porosity $\varepsilon_T=0.60$ is 2.5 mL), which will suffer significantly less from a large system volume.

The aim of this study is to assess the intrinsic performance of 5 μm core–shell particles (150 × 4.6 mm and 250 × 4.6 mm) on a conventional HPLC without any modifications made to decrease its volume. The performance of these columns is compared to that of a 250 × 4.6 mm fully porous 5 μm column using the kinetic plot method, both under isocratic and gradient conditions. After an intrinsic column comparison with test compounds, the performance of the columns is assessed for the analysis of griseofulvin (GF) and its impurities.

GF is an orally administered antimycotic agent that has been on the market for more than forty years [9]. The drug is still highly relevant due to its low price, making it specifically interesting for developing countries. A method for the determination of GF and its impurities has only recently been developed on a traditional 250 × 4.6 mm, 5 μm fully porous column [10]. Conventional columns and equipment were chosen on purpose to make the method applicable in developing countries where GF is mostly administered. It is investigated whether the use of 5 μm core–shell particle columns can yield a significant increase in resolution and/or decrease in analysis time, without having to re-optimize the method significantly.

Finally, the loadability of the core–shell columns is compared to that of the fully porous particle column. Loadability is especially important in impurity profiling, where a high column loadability can increase the sensitivity of a method significantly. The loadability of sub-3 μm shell particles was demonstrated to be comparable to that of sub-2 μm fully porous particles, as the porous volume of the former still constitutes up to 60–75% of the total volume of the particle [11]. Loadability can be assessed for different columns by comparing the sample loading capacity $\omega_{0.5}$ or concentration $C_{0.5}$, leading to a loss of half the efficiency which is obtained under infinite dilution conditions [12]. This comparison can, however, only be made when the columns being compared (1) have exactly the same efficiency under infinite dilution conditions, (2) are operated using a mobile phase composition leading to the same retention factor for the compound under consideration, (3) the concentrations or masses being injected are scaled to the stationary phase volume, and (4) the ratio of injection time (volume) to column void time (t_0) is small ($<1/35$) [13].

In this paper, a much more practical approach to compare the loadability of core–shell and fully porous columns is proposed. Plots of the resolution between GF and its closest impurity versus the signal-to-noise ratio (S/N) for the smallest impurity are determined at concentrations ranging between 0.25 mg/mL and 10 mg/mL. The S/N ratio for the smallest impurity is an indication for the sensitivity of the column and can be increased by injecting a higher concentration. Columns which are easily overloaded will, however, suffer more from band broadening at higher concentrations which can result in a decreased resolution for GF and its closest impurity.

2. Theory

Kinetic plots denote the column void time (t_0) or the analysis time (t_R) versus the plate count (N) or peak capacity (n_p) and can be constructed for chromatographic columns and/or systems with any kind of morphology and/or physicochemical property. They can be obtained without any iterative procedure, by transforming experimental plate-height data (H versus u_0, with u_0 the linear velocity of the mobile phase) into corresponding values of t_0 versus N, using the following two equations:

$$t_0 = \frac{\Delta P_{max}}{\eta}\left(\frac{K_{v0}}{u_0{}^2}\right) \quad (1)$$

$$N = \frac{\Delta P_{max}}{\eta}\left(\frac{K_{v0}}{u_0 H}\right) \quad (2)$$

In these equations, η and K_{v0} stand for the mobile-phase viscosity and the column permeability, respectively, while ΔP_{max} is the maximum column or instrument pressure which allows obtaining the ultimate performance limits of the columns or supports under consideration. From t_0 and N, other important quantities such as t_R, n_p and resolution (R_s) can easily be derived [14,15]. As can be deduced from Eqs. (1) and (2), kinetic plots combine information on column efficiency and permeability and therefore provide a more complete picture of column performance than what is for example obtained using a classical van Deemter curve.

Eqs. (1) and (2) have been demonstrated to work well under isocratic separation conditions, but are not that easily applied to gradient elution, as column plate heights are more difficult to define accurately under gradient conditions. It has, however, been shown that kinetic plots can also be constructed immediately from experimentally determined t_0 (or t_R) versus N (or n_p) – data, obtained at different flow rates on a column with a fixed length, by transforming these data using a length elongation factor (λ):

$$t_{R,\,KPL} = \lambda t_{R,\,exp} \quad (3)$$

$$n_{p,\,KPL} = 1 + \sqrt{\lambda}(n_{p,\,exp} - 1) \quad (4)$$

$$N_{KPL} = \lambda N_{exp} \quad (5)$$

In these equations, the subscript "exp" refers to the experimentally determined data points, whereas "KPL" represents the corresponding data points on the kinetic plot curve. The length elongation factor $\lambda = \Delta P_{max}/\Delta P_{exp}$, denotes the ratio of the maximum available pressure (on the column or the system) to the pressure recorded at the specific flow rate at which each of the t_0 versus N-data points were obtained, and assures that each point on the kinetic plot curve is reached at the kinetic optimum.

The advantage of Eqs. (3)–(5) is that they hold both under isocratic and gradient conditions. For gradient conditions, data must be collected by applying the same relative mobile-phase gradient history [16]. This can be achieved by applying the same ratio of t_G/t_0 and t_{delay}/t_0 at each flow rate and on every evaluated column length (t_G is the gradient time and t_{delay} the gradient delay time).

3. Experimental

3.1. Chemicals and reagents

HPLC gradient grade acetonitrile (ACN) was obtained from Fisher Scientific (Leicestershire, UK) and formic acid (FA) from Biosolve Ltd. (Valkenswaard, The Netherlands). HPLC grade water was prepared in the laboratory using a Milli-Q gradient water purification system (Millipore, Bedford, MA, USA). Uracil (> 99%) was purchased from Janssen Chimica (Geel, Belgium). Acetanilide, acetophenone, 3-methyl acetophenone, propiophenone, butyrophenone, benzophenone valerophenone, hexaphenone, heptaphenone and octaphenone were purchased from Sigma-Aldrich (Steinheim, Germany).

3.2. Instrumentation and columns

The LC system from Dionex Softron GmbH (Germering, Germany) was equipped with a high pressure pump (P680ALPG), autosampler (ASI-100T) and UV/VIS detector (UVD170U) with a 14 μL flow cell. The gradient dwell volume of the system was determined to be 1.6 mL, while the system volume (from injector to detector) was determined to be 89 μL. For data processing and acquisition, Chromeleon software version 6.80 from Dionex (Sunnyvale, CA, USA) was used. The column was kept in a water bath at a temperature of 30 °C using a Julabo EM immersion thermostat (Seelbach, Germany). A pH meter from Metrohm (Herisau, Switzerland) was used to measure the pH of the mobile phase. Chromatographic separations were done on a fully porous Discovery C_{18} column (250 × 4.6 mm, 5 μm) and two core–shell Ascentis Express C_{18} columns (250 × 4.6 mm, 5 μm and 150 × 4.6 mm, 5 μm) obtained from Supelco (Sigma-Aldrich, Bellefonte, PA, USA).

3.3. Samples and chromatographic conditions

To evaluate the isocratic performance of the fully porous and core–shell particle columns, a solution of uracil, propiophenone, butyrophenone and benzophenone (10 μg/mL each) was prepared in the mobile phase (mixture of ACN/H_2O, see Table 1). The amount of ACN in the mobile phase was adjusted for each column to keep the retention factor of propiophenone (k=2.8), butyrophenone (k=6.1) and benzophenone (k=8.1) constant on all columns (Table 1). The asymmetry of the peaks on the three columns was also evaluated and found to be in the range of 1.00–1.28. Plate counts were calculated from the peak widths determined at half the peak height according to the European Pharmacopoeia [17] without correcting for the system variance (σ^2_{ext}). This was done on purpose to obtain the column performance as available on a conventional HPLC system. The system variances and system void time (t_{ext}) were assessed in a separate experiment by replacing the column with a zero-dead volume union.

Average column permeabilities (K_{v0}) were assessed from the backpressures (ΔP) measured at each flow rate considered during the van Deemter experiments:

$$K_{v0} = \frac{u_0 \eta L}{\Delta P} \quad (6)$$

where η is the mobile phase viscosity (Pa s), determined according to [18], and L the column length (m). In this case, ΔP was corrected for the system pressure and the linear velocity u_0 ($u_0 = L/(t_0 - t_{ext})$) for the system void time to obtain the intrinsic column permeabilities.

The gradient kinetic performance of the columns was assessed using a solution of 10 μg/mL each of acetanilide, acetophenone, 3-methyl acetophenone, propiophenone, butyrophenone, benzophenone valerophenone, hexaphenone, heptaphenone and octaphenone, prepared in 50:50 (v/v) ACN/H_2O. All gradient experiments for the alkylphenone solution were performed using H_2O as mobile phase A and ACN as mobile phase B. The gradient start concentration (ϕ_0), end concentration (ϕ_e) and steepness (related to the gradient time t_G) were adapted for each column to keep the ratio of t_G/t_0 constant at 12 and the apparent retention factors (k) for the second eluting compound (acetophenone) and last eluting compound (octanophenone) at k=2.0 and k=12.0, respectively (Table 1). The ratio of t_{delay}/t_0 ($t_{delay} = t_{dwell} + t_{isocratic\ hold}$, with t_{delay} the total delay time, t_{dwell} the system dwell time and $t_{isocratic\ hold}$ the time of the applied isocratic hold at the start of the gradient) was kept constant as well. The column void time (t_0) of each column was determined from the elution time of uracil, corrected for the system void time (t_{ext}, obtained by replacing the column by a zero-dead volume connector). The obtained hold-up times are shown in Table 1.

The performance of the columns was further evaluated using GF and its impurities obtained from Ludeco (Brussels, Belgium) and Aca Pharma (Waregem, Belgium). The chemical structures of GF and its main impurities are shown in Table 2. The mobile phase consisted of a mixture of mobile phase A (water – 0.1% formic acid pH 4.5, 80:20 v/v) and B (ACN – water – 0.1% formic acid pH 4.5, 65:15:20 v/v/v) pumped at a flow rate of 1.0 mL/min. The original gradient program applied on the Discovery C_{18} column is shown in Table S-1 in Supplementary information [10]. To maintain the selectivity of the separation on the other evaluated columns, the ratios of t_G/t_0 and t_{delay}/t_0 were again kept constant on all columns. After a first evaluation of the obtained separations, the initial (ϕ_0) and final (ϕ_e) percentages of ACN were adapted slightly to maintain a constant retention factor for GF (k=5.4) on all columns. UV detection was performed at 290 nm. The final gradient programs obtained in this way for the Ascentis Express C_{18} columns are also shown in Table S-1. Table 3 shows the gradients that were used at the maximum system pressure (P_{max}=400 bar), always

Table 1
Characteristics of the columns used in the study and their permeability under experimental mobile phase conditions.

Column	Particle type	I.D. (mm)	length (mm)	d_p (μm)	K_{v0} (m^2) ($\times 10^{-14}$)	t_0 (min)[a]	% ACN	Propiophenone		Butyrophenone		Benzophenone		Gradient conditions	
								k (± RSD)	H_{min} (μm)	k (± RSD)	H_{min} (μm)	k (± RSD)	H_{min} (μm)	ϕ_0	ϕ_{end}
Ascentis Express C_{18}	SP	4.6	150	5	3.05	1.09	42.5	2.8 ± 0.1	8.0	6.2 ± 0.1	7.4	8.1 ± 0.1	7.3	0.37	0.83
Ascentis Express C_{18}	SP	4.6	250	5	4.08	1.82	42.5	2.7 ± 0.1	8.7	6.1 ± 0.1	8.2	7.9 ± 0.1	8.2	0.37	0.83
Discovery C_{18}	FP	4.6	250	5	3.27	2.62	40.0	2.9 ± 0.1	11.4	6.1 ± 0.1	11.7	8.2 ± 0.1	11.9	0.36	0.77

SP: Superficially porous; FP: Fully porous; % ACN: amount of ACN used to obtain $k \approx 6$ (butyrophenone) in isocratic conditions.

[a] t_0 obtained at a flow rate of 1.0 mL/min.

Table 2
Chemical structure of griseofulvin and its main impurities.

Chemical name	Chemical structure
Griseofulvin	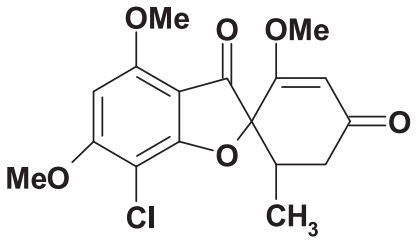
Griseofulvic acid	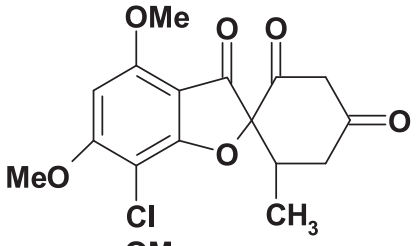
Dechlorogriseofulvin	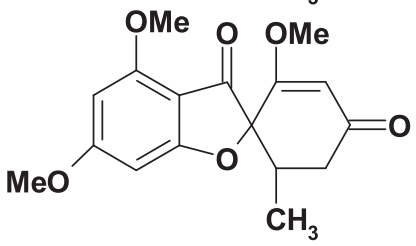
Dehydrogriseofulvin	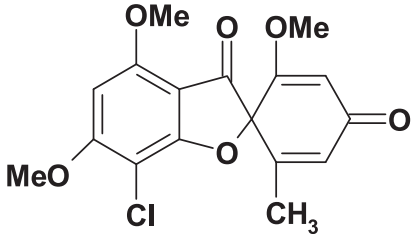

Table 3
Gradient programs applied for the separation of GF and its impurities on the 3 investigated columns at the maximum column pressure. Applied flow rates are indicated.

Discovery 25 cm (*F*=2.3 mL/min)		**Ascentis Express 25 cm (*F*=2.0 mL/min)**		**Ascentis Express 15 cm (*F*=2.5 mL/min)**	
Time (min)	Mobile phase B (% v/v)	Time (min)	Mobile phase B (% v/v)	Time (min)	Mobile phase B (% v/v)
0	50	0	49.5	0	49.5
1.30	50	0.8	49.5	0.13	49.5
5.65	60	4.28	60	1.79	60
6.96	90	5.32	90	2.29	90
8.70	90	6.71	90	2.96	90
10.43	50	8.10	49.5	3.62	49.5
13.04	50	10.18	49.5	4.62	49.5

keeping the ratios of t_G/t_0 and t_{delay}/t_0 constant to maintain the selectivity of the separation.

For the mass loadability study, 16 concentrations of GF and its impurities (0.25, 0.5, 0.75, 1.0, 1.25, 1.5, 1.75, 2.0, 3.0, 4.0, 5.0, 6.0, 7.0, 8.0, 9.0 and 10.0 mg/mL) were prepared. The same gradient conditions were used as described in the previous paragraph. Peak variances and retention times of the resulting peaks were determined using the method of moments to calculate the resolution (R_s) between GF and its closest eluting impurity as follows:

$$R_s = \frac{1}{2}\frac{\mu_{1,\ peak_2} - \mu_{1,\ peak_1}}{\left(\sqrt{\mu_{2,\ peak_1}} + \sqrt{\mu_{2,\ peak_2}}\right)} \quad (7)$$

wherein μ_1 refers to the first moment, μ_2 to the second moment, $peak_1$ to the first eluting peak of the critical pair and $peak_2$ to the last eluting peak of the critical pair. The retention time is equal to the first moment.

For all experiments, the injection volume was scaled according to the hold-up volume of the column (proportional with t_0). This resulted in an injection volume of 10 μL for the Discovery C_{18} (250 × 4.6 mm) column [10], 7.0 μL for the Ascentis Express C_{18} (250 × 4.6 mm) column and 4.12 μL for the Ascentis Express C_{18} (150 × 4.6 mm) column.

4. Results and discussion

4.1. Van Deemter plot comparison

Uncorrected van Deemter plots of the measured plate height (H) as a function of linear velocity (u_0) for the Ascentis Express C_{18} (SP) and Discovery C_{18} (FP) columns are shown in Fig. 1. The data were not corrected on purpose, to demonstrate the actual column efficiencies that can be obtained on a conventional HPLC system (system volume=89 μL). System variances were determined in a separate experiment and were < 25% of the total variance for

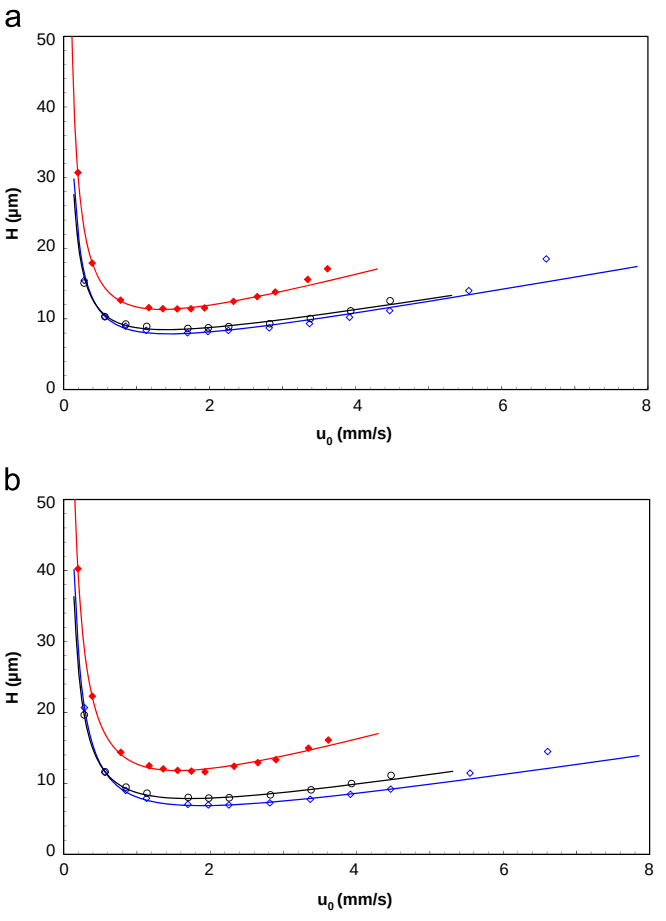

Fig. 1. van Deemter curves of plate height (H) versus linear velocity (u_0) for (a) propiophenone (k=2.8) and (b) benzophenone (k=8.1) for columns packed with superficially porous particles: Ascentis Express C_{18} 150 × 4.6 mm, 5 μm (◊), Ascentis Express C_{18} 250 × 4.6 mm, 5 μm (o) and fully porous particles: Discovery C_{18} 250 × 4.6 mm, 5 μm (♦). Mobile phase conditions given in Table 1.

propiophenone (k=2.8), <8% of the total variance for butyrophenone (k=6.2) and <5% of the total variance for benzophenone (k=8.1) on the 15 cm Ascentis Express C_{18} column at all evaluated flow rates. For the 25 cm Ascentis Express C_{18} column, these values were slightly lower and <15% of the total variance for propiophenone (k=2.7), <5% of the total variance for butyrophenone (k=6.1) and <3% of the total variance for benzophenone (k=7.9). Finally, for the Discovery C_{18} column the system variance was <6% of the total variance for propiophenone (k=2.9), <2% of the total variance for butyrophenone (k=6.1) and <1% of the total variance for benzophenone (k=8.2). These results indicate that the volume of the system has a non-negligible effect on the efficiency of the superficially porous (SP) columns for compounds with k<5.0, despite the large hold-up volume of the columns.

Despite the larger extra-column influence, Fig. 1 shows that the SP columns attain lower plate heights and hence higher efficiencies than the FP column over the entire range of studied velocities for all investigated compounds (k=2.8 to k=8.1, the van Deemter curves for butyrophenone are shown in Supplementary information, Fig. S-1). The van Deemter curves obtained on the 15 cm and 25 cm SP particles moreover coincide rather well, be it that the 15 cm column performs slightly better than the 25 cm column (Table 1). Broeckhoven et al. [3] reported a similar trend for the efficiency comparison of FP and SP 5 μm particles. The plate height minima (H_{min}) for the SP particles decrease by a factor of 1.3–1.6 compared to the FP particles as shown in Table 1.

The slopes of the C-term dominated region of the curves moreover show a slightly larger efficiency loss as the flow rate is increased beyond the optimum linear velocity for the FP column in comparison with the SP columns. Therefore faster flow rates can be used on the SP columns resulting in only a small loss of efficiency, which allows decreasing the analysis time. The low C-term of the SP columns results from the much lower A-term contribution in the high-velocity range in comparison with the FP particles [3].

4.2. Kinetic plot comparison: t_0 versus N

For a fair comparison of column performance, not only column efficiency (cfr. van Deemter plots and minimum plate heights) should be regarded, but also the backpressure of the column (ΔP) at a certain flow rate should be taken into consideration. For this purpose, column permeabilities (K_{v0}) were assessed from the backpressures measured at each flow rate considered during the plate height measurements. The obtained values are shown in Table 1 and demonstrate relatively similar permeability values for the SP columns in comparison with the FP column.

From the van Deemter plots in Fig. 1 and the permeability values in Table 1, kinetic plots of t_0 versus N were subsequently constructed using Eqs. (1) and (2) for a maximum pressure of 400 bar. The obtained curves are shown in Fig. 2 and again reveal a superior performance for the 5 μm SP particles in comparison with the 5 μm FP particles over the entire range of separations and for all investigated compounds (k=2.8 to k=8.1, the plots for butyrophenone are shown in Supplementary information Fig. S-2). The plots obtained for both superficially porous particles coincide very well, as the slightly better efficiency of the 15 cm SP column is now compensated by its lower permeability. From the plots in Fig. 2, it can be assessed that for the practical range of efficiencies (i.e., the plate counts which are required to perform most separations; N=10,000–100,000), a gain in analysis time of roughly 1.5–2.5 can be achieved using the SP particles in comparison to the FP particles on conventional HPLC instrumentation, when both particle types are evaluated at the same pressure. As an example, the arrows in Fig. 2 denote the required analysis times (proportional to t_0, considering $t_R=t_0(1+k)$ and the retention times are the same

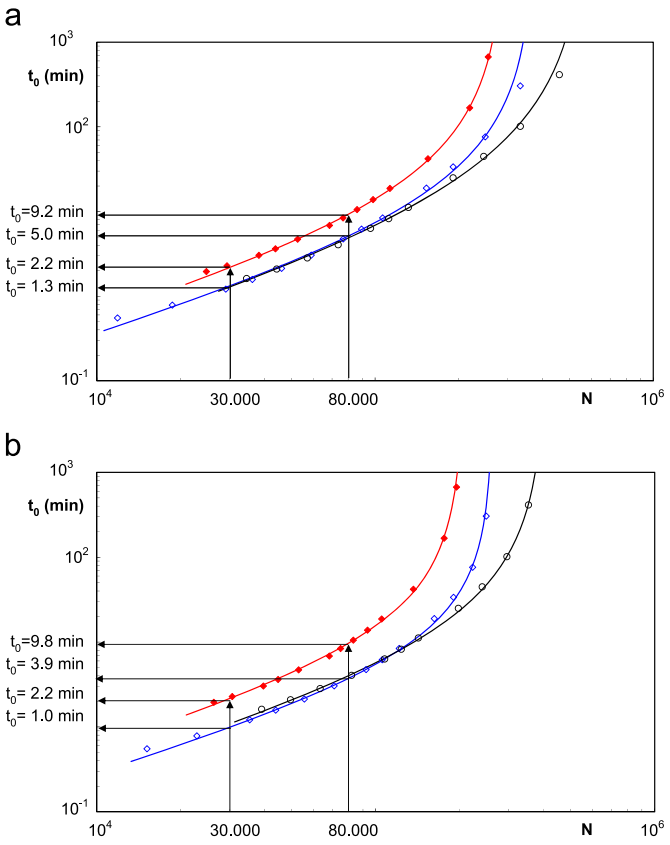

Fig. 2. Kinetic plots of t_0 versus N (ΔP_{max}=400 bar) for (a) propiophenone (k=2.8) and (b) benzophenone (k=8.1). Same columns and symbols as in Fig. 1. The arrows indicate the t_0-times corresponding with a plate count of 30,000 and 80,000.

on all columns) on SP and FP particles to obtain plate counts of N=30,000 and N=80,000, respectively.

4.3. Kinetic plot comparison: L versus N

Fig. 3 shows the corresponding lengths which are required to obtain the plate counts in Figs. 2 and S-2. For simplicity sake, only the data for butyrophenone are shown here. These column lengths are derived from the plate counts and can be obtained by the following calculation for each data point:

$$L = NH = \frac{\Delta P_{max} K_{v0}}{\eta u_0} \quad (8)$$

or, even simpler, as

$$L_{KPL} = \lambda L_{exp} \quad (9)$$

using the length elongation factor.

Due to the higher efficiency of the SP particles, identical plate counts can be obtained in shorter columns compared to the FP column, which will moreover be operated at higher velocities at the maximum pressure, resulting in the shorter analysis times in Figs. 2 and S-2. On average, columns which are a factor 1.5–1.6 shorter for the SP particles in comparison with the FP particles are required to obtain a certain plate count. As an example, the arrows in Fig. 3 compare the column lengths required to obtain plate counts of N=30,000 and N=80,000 on SP and FP particles, respectively.

4.4. Kinetic plot comparison under gradient conditions: t_0 versus n_p

The peak capacity of the 3 columns was also compared as a function of analysis time in gradient conditions. The peak capacity

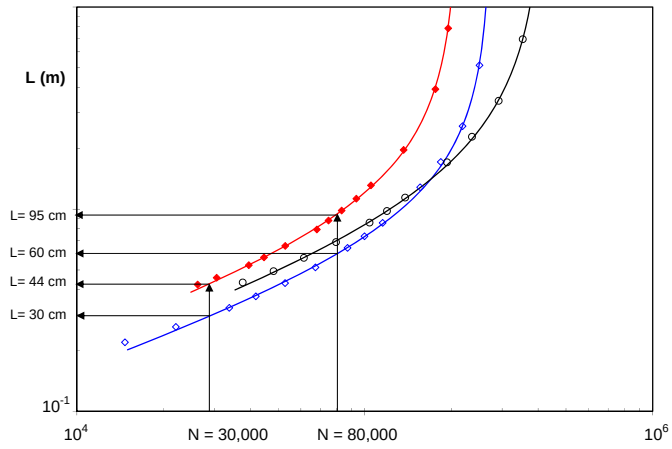

Fig. 3. Kinetic plots of L versus N (ΔP_{max}=400 bar) for butyrophenone (k=6.1). Same columns and symbols as in Fig. 1. The arrows indicate the column lengths required to obtain a plate count of 30,000 and 80,000.

$n_{p,exp}$ was first determined at each considered flow rate as follows:

$$n_{p,exp} = 1 + \sum_{i=1}^{n} \frac{t_{R,i} - t_{R,i-1}}{4\sigma_{t,i}} \quad (10)$$

wherein $4\sigma_t$ is the peak width at the base, and subsequently translated into the data represented in the kinetic plots in Fig. 4 according to Eq. (3).

When peak variances and analysis times were not corrected for the system contribution, the plots in Fig. 4a were obtained. In contrast to the uncorrected isocratic kinetic plots in Fig. 2 where the plots of the SP particles coincide, a larger discrepancy is now observed for the gradient kinetic plots of the 15 cm and the 25 cm Ascentis Express C_{18} columns. This is a direct result of the much smaller peak volumes ($4\sigma_V$) in gradient elution (e.g. between 100 and 170 μl for the 15 cm Ascentis Express C_{18} column) than in isocratic elution (between 130 and 450 μl), making the former much more sensitive to extra-column band broadening effects. However, for gradient elution the pre-column band broadening contributes only insignificantly to the peak width due to the focusing effect at the head of the column. To explain the observed phenomena, the extra-column band broadening was experimentally determined by replacing the column by a zero-dead volume connector and injecting an unretained marker under the same gradient conditions as for the actual column measurements. Subsequently, the contribution of the pre-column band broadening was calculated and compared to the experimentally obtained values. The peak variance ($\sigma_{V,inj}^2$) due to the finite volume (V_{inj}) can generally be written as [19]:

$$\sigma_{V,\,inj}^2 = \frac{V_{inj}^2}{\theta} \quad (11a)$$

with θ a parameter with a typical value between 5 and 12. The dispersion in the pre-column tubing ($\sigma_{V,\,tub}^2$) on the other hand can, using the insights in the steady-state and the transient phase of the axial dispersion process in open tubes obtained in [20], be written as

$$\sigma_{V,\,tub}^2 = \frac{L_{tub} d_{tub}^2}{384 D_{mol}} F \left[1 - \frac{(1 - e^{-\alpha L_{tub}})}{\alpha L_{tub}}\right] \quad (11b)$$

where L_{tub} and d_{tub} are the tubing length and diameter, F is the volumetric flow rate (m³/s), D_{mol} the molecular diffusion coefficient (m²/s), and $\alpha = 15\pi D_{mol}/F$ (the factor 15 originates from the approximate geometrical proportionality constant 60 derived in [20] for the case of a laminar parabolic flow). Calculating the sum of these contributions for the employed injection volume (maximum 10 μl) and inlet tubing (L_{tub}=40 cm, d_{tub}=125 μm), this

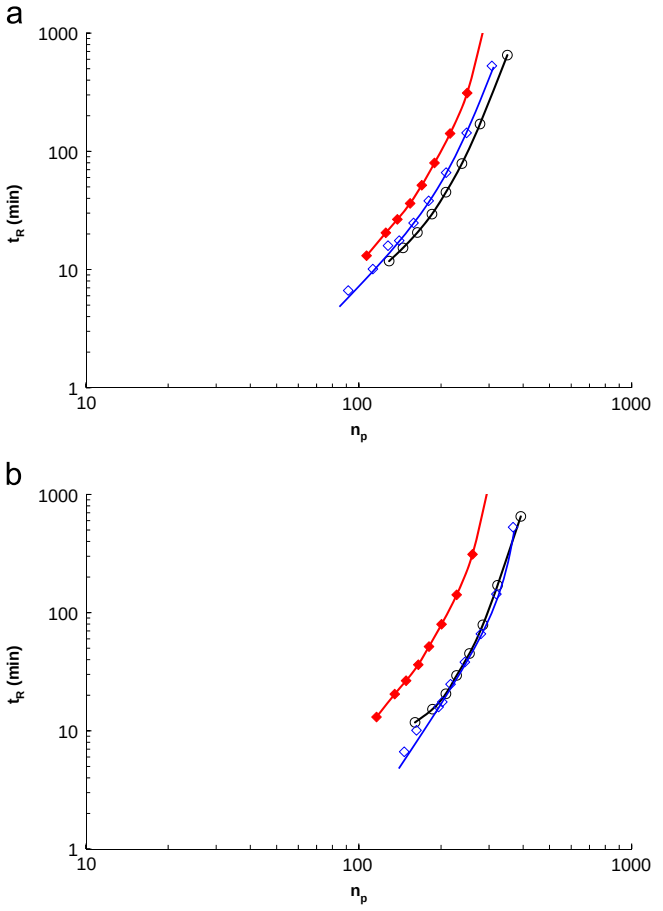

Fig. 4. Gradient kinetic plot of column void time (t_0) versus peak capacity n_p (ΔP_{max}=400 bar) for typical alkylphenones with apparent retention factors between k=2 and k=12. Plots are (a) not corrected for the system contribution, and (b) corrected for the system contribution. Same columns and symbols as in Fig. 1.

accounts, even in the most limiting cases, to only 10% of the total experimentally measured extra-column band broadening (with $D_{mol} = 7.8 \times 10^{-10}$ m²/s for benzophenone in a 50/50%v/v mobile phase at 30 °C calculated according to the Wilke-Chang equation [21]). This indicates that the majority of the extra-column dispersion occurs after the column and strongly affects the narrow peaks eluting from the column in gradient elution. Due to the smaller column volume of the 15 cm Ascentis Express C_{18} column compared to the 25 cm column, the former is more strongly affected, resulting in the discrepancy between their kinetic performance limits in Fig. 4a. Correcting for the extra-column contribution, the curves presented in Fig. 4b are obtained, which once again show a good agreement in kinetic performance between the 15 and 25 cm column.

The above discussion shows that even for relatively long, large ID columns with large particles, the effects of extra-column band broadening can be important, especially in gradient elution when a significant dispersion volume is located after the column. In the employed experimental set-up, this was mainly due to the larger inlet tubing of the detector (L_{tub}=40 cm, d_{tub}=250 μm) and detector cell volume (14 μl), which were inherent to the system. Both superficially porous columns, however, still outperform the fully porous column over the entire range of peak capacities – even when no system correction is made- and lead to a gain in analysis time of 1.5–2.5 for a fixed peak capacity.

Gradient kinetic plots of column length (L) versus peak capacity furthermore indicated that the same peak capacity can be obtained

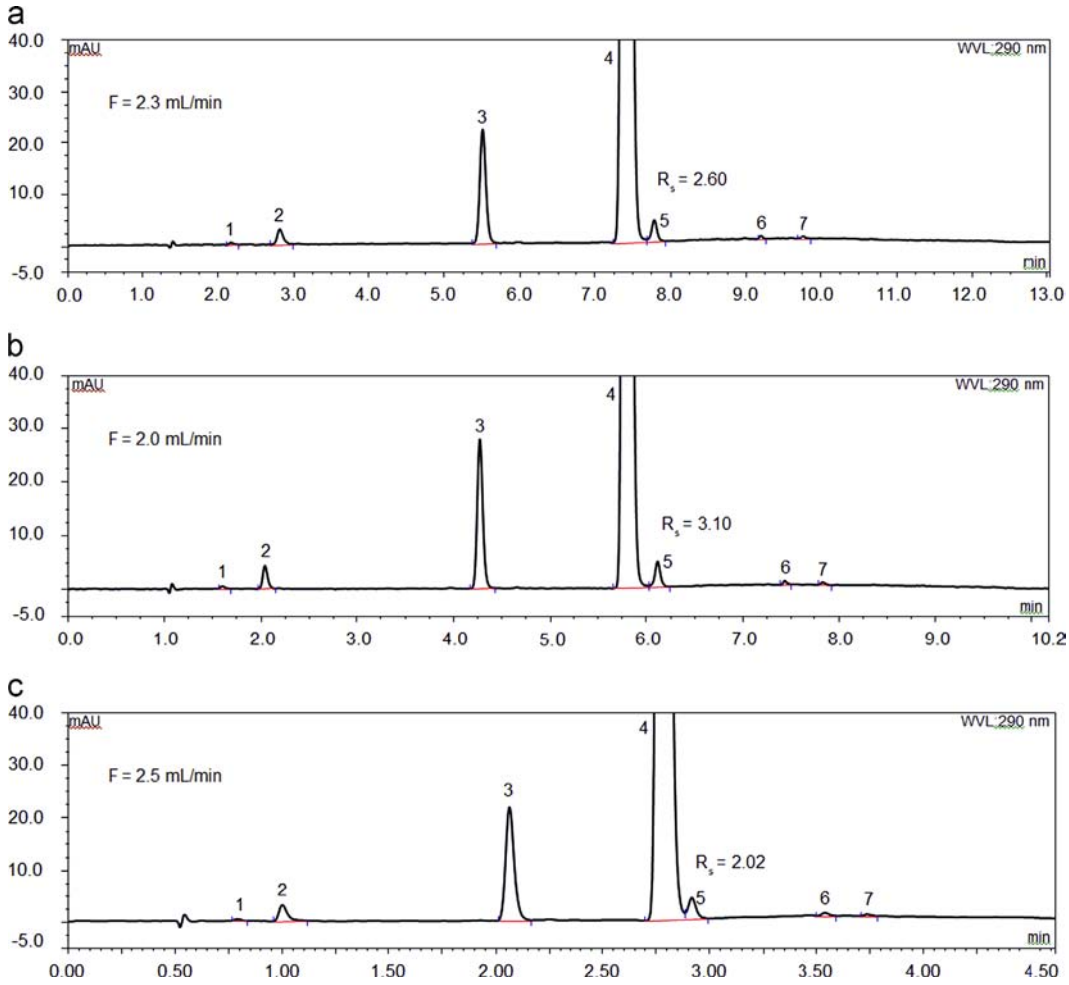

Fig. 5. Chromatograms obtained for griseofulvin and its main impurities at the maximum column pressure on (a) the 25 cm Discovery C_{18} column, (b) the 25 cm Ascentis Express C_{18} column and (c) the 15 cm Ascentis Express C_{18} column. Gradient conditions see Table 3. Peak identification: 1: Unknown, 2: Griseofulvic acid, 3: Dechlorogriseofulvin, 4: Griseofulvin, 5: Dehydrogriseofulvin, 6: Unknown and 7: Unknown.

on a SP column which is some 1.5 times shorter than its FP counterpart (data not shown). For the columns investigated in this study, these data indicate that a similar peak capacity should be obtained on a 25 cm FP and 18 cm SP column, and that the latter would lead to a decrease in analysis time with a factor of ~2 when both columns would be evaluated at the same maximum pressure.

4.5. Application: separation of GF and impurities

The chromatographic performance of both particle types was further compared for the separation of a pharmaceutical compound (griseofulvin) and its impurities (Fig. S-3). The original gradient conditions for the FP column were adapted in such a way for the SP columns, that a constant ratio of t_G/t_0 and t_{delay}/t_0 was maintained on all columns. This resulted in a similar selectivity for GF and its impurities (the system suitability test results of the method for the analysis of GF and its impurities are shown in Table S-2 in Supplementary information). From a practical point of view, all columns were first operated at the same flow rate of 1 mL/min, as this is the most common flow rate for pharmaceutical analyses on large bore columns. The resulting chromatograms are shown in Fig. S-3 in Supplementary information. When switching from a 25 cm FP column to a 25 cm SP column, the total analysis time decreases with a factor of ~1.5 due to the smaller hold-up volume of the SP column (Table 1). The larger performance of the 25 cm SP column, moreover leads to an increase in resolution for the critical peak pair from R_s=3.2 (FP column) to R_s=3.7 (SP column). Comparing the chromatograms obtained on the 25 cm FP and the 15 cm SP column, the analysis time is now reduced with a factor of 2.5, while the resolution between GF and its closest impurity is slightly lower than on the FP column (R_s=2.7 versus R_s=3.2), but still sufficient for baseline separation.

To verify the observations made from the kinetic plots in Section 4.4, all columns were also operated at the maximum instrument pressure. The obtained chromatograms are shown in Fig. 5. Unfortunately, a SP column with a length of 18 cm was not available, but the chromatograms in Fig. 5 show that a decrease in analysis time of some 1.3 times is obtained on the 25 cm SP column and of some 2.7 times on the 15 cm SP column, compared to the FP column. The resolution on the 25 cm SP column is larger than on the FP column (R_s=3.1 versus 2.6), while that on the 15 cm SP column is lower compared to the FP column (R_s=2.0 versus 2.6). Taking into account that some slight selectivity differences will always be present on different columns, it can be deduced from these results that a SP column with a length of 18 cm would indeed lead to a comparable resolution as obtained on the FP column, but in an analysis time which is some 2.0 times lower, as predicted by the kinetic plot curves.

4.6. Loadability comparison for columns of equal efficiency

To fulfill the requirements for a correct comparison of column loadability (as described in the introduction), the gradients on all evaluated columns were adapted to yield a constant retention

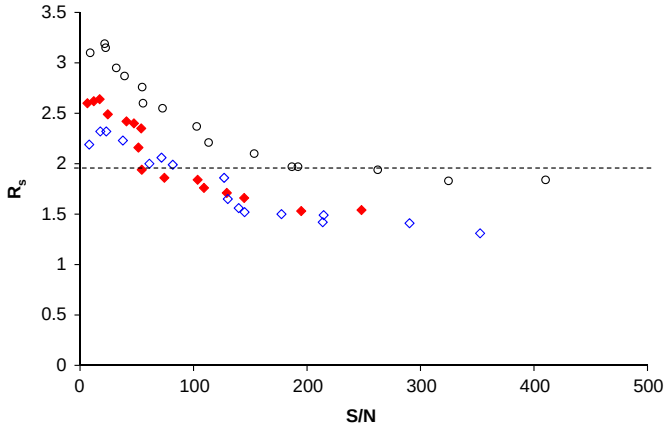

Fig. 6. Plots of resolution between griseofulvin and its closest impurity versus the signal-to-noise ratio for the smallest impurity of griseofulvin for different concentrations of griseofulvin. Same symbols as in Fig. 1.

factor for GF. Furthermore, the 25 cm FP column and the 15 cm SP column were selected for the loadability comparison as they yielded a similar performance as can be deduced from Table 1 (N=21,000 plates). To evaluate column loadability in a practically relevant way, the resolution (R_s) between GF and its closest impurity was compared as a function of the signal-to-noise ratio (S/N) for the smallest impurity. Columns with a lower efficiency, will require a higher sample concentration to obtain a sufficiently high signal-to-noise ratio (S/N > 10) for quantitation of the smallest impurity. When this concentration becomes too large, the resolution between the API and its nearest impurity might get compromised due to band broadening resulting from column overloading. The results in Fig. 6 demonstrate that the 15 cm SP column yields a very similar resolution between GF and its nearest impurity as the 25 cm FP column, for S/N ratios of the smallest impurity between 10 and 100. The resolution on the SP column moreover remains ≥2.0 (which is the typical minimum resolution required between an API and its impurities in pharmaceutical analyses [22]) for this S/N range. It can therefore be deduced that the sensitivity of the SP column is not significantly compromised as a result of its reduced porous volume in comparison with its FP counterpart, when both columns yield a similar efficiency. The 25 cm SP column leads to a higher S/N ratio for a fixed resolution and hence a higher sensitivity in comparison with the two other columns, which can be attributed to its higher efficiency. Depending on the application, the analyst could therefore decide to switch from a 25 cm FP column to a 25 cm SP column (when a high sensitivity is the main goal and the analysis time does not have to be reduced drastically) or to a 15 cm SP column (when a decrease in analysis time is envisaged and a similar sensitivity as on the FP column can be tolerated).

5. Conclusion

In the present study, the performance of 5 μm SP particles was compared to that of FP 5 μm particles in terms of efficiency, separation performance and loadability on a conventional HPLC system. The van Deemter and kinetic plots show that 5 μm SP particles provide a superior kinetic performance compared to 5 μm FP particles over the entire relevant range of separation conditions using alkylphenones as test compounds. Compared to the FP particles, the SP particles give better efficiency at higher flow rates thus allowing to decrease the analysis time. The Ascentis Express C_{18} columns also perform better than the FP Discovery C_{18} column in the entire range of obtainable peak capacities under gradient conditions, despite the fact that the conventional system set-up (with large flow cell) leads to a larger relative system contribution for the SP columns than for the FP columns under gradient conditions. Moreover, the SP particles show better separation efficiency for griseofulvin and its impurities, both at a conventional flow rate of 1 mL/min and at maximum column pressure, and allow obtaining a decrease in analysis time of a factor of 2 under both conditions. It is demonstrated that the sensitivity attainable on the SP particles is not compromised in comparison to the FP particles. In fact, the 15 cm SP column yields a similar sensitivity to the 25 cm FP column, while that of the 25 cm SP column is significantly higher due to its higher intrinsic efficiency. The results presented here demonstrate that switching from a 25 cm FP column to a SP column will always be beneficial, either in terms of sensitivity and resolution, while maintaining a rather similar analysis time (25 cm SP column) or in terms of analysis time, while maintaining a similar sensitivity and resolution (15 cm SP column), and without having to make any modifications to the system.

Acknowledgments

The authors would like to thank the Interfaculty Council for Development Co-operation (IRO), KU Leuven, for financial support. Dave Bell from Sigma-Aldrich is kindly thanked for the gift of the Ascentis Express C_{18} columns.

Appendix A. Supporting information

Supplementary data associated with this article can be found in the online version at http://dx.doi.org/10.1016/j.talanta.2014.01.050.

References

[1] F. Gritti, G. Guiochon, J. Chromatogr. A 1280 (2013) 35–50.
[2] J. DeStefano, A. Schuster, J. Lawhorn, J. Kirkland, J. Chromatogr. A 1258 (2012) 76–83.
[3] K. Broeckhoven, D. Cabooter, G. Desmet, J. Pharm. Anal. 3 (2013) 313.
[4] F. Gritti, A. Cavazzini, N. Marchetti, G. Guiochon, J. Chromatogr. A 1157 (2007) 289–303.
[5] J. Ruta, D. Zurlino, C. Grivel, S. Heinisch, J-L. Veuthey, D. Guillarme, J. Chromatogr. A 1228 (2012) 221–231.
[6] D. Cabooter, F. Lestremau, F. Lynen, P. Sandra, G. Desmet, J. Chromatogr. A 1212 (2008) 23–34.
[7] F. Gritti, C.A. Sanchez, T. Farkas, G. Guiochon, J. Chromatogr. A 1217 (2010) 3000–3012.
[8] Y. Vanderheyden, D. Cabooter, G. Desmet, K. Broeckhoven, J. Chromatogr. A 1312 (2013) 80–86.
[9] M. DevelouxGriseofulvin, Ann. Dermatol. Venereol. 128 (2001) 1317–1325.
[10] G. Kahsay, A. Adegoke, A. Van Schepdael, E. Adams, J. Pharm. Biomed. Anal. 80 (2013) 9–17.
[11] J. Dai, P.W. Car, D.V. McCalley, J. Chromatogr. A 1216 (2009) 2474–2482.
[12] D.V. McCalley, J. Chromatogr. A 1218 (2011) 2887–2897.
[13] F. Gritti, G. Guiochon, J. Chromatogr. A 1254 (2012) 30.
[14] A. Fanigliulo, D. Cabooter, G. Bellazzi, B. Allieri, A. Rottigni, G. Desmet, J. Chromatogr. A 1218 (2011) 3351–3359.
[15] G. Desmet, D. Clicq, P. Gzil, Anal. Chem. 77 (2005) 4058–4070.
[16] K. Broeckhoven, D. Cabooter, F. Lynen, P. Sandra, G. Desmet, J. Chromatogr. A 1217 (2010) 2787.
[17] European Pharmacopoeia 7th edition, vol. 2. European Directorate for the Quality of Medicines and Healthcare, Council of Europe, Strasbourg, 2011.
[18] J. Li, P.W. Carr, Anal. Chem. 69 (1997) 2530.
[19] H. Poppe, Chromatography, fundamentals and applicatons of chromatograph and related differential migratin methods, in: E. Heftmann (Ed.), Journal of Chromatography Library, Elsevier,Amsterdam, The Netherlands, 1992, pp. 151–225.
[20] K. Broeckhoven, G. Desmet, J. Chromatogr. A 1216 (2009) 1325–1337.
[21] C.R. Wilke, P. Chang, AIChE J. 1 (1955) 264.
[22] Center for Drug Evaluation and Research, U.S. Food and Drug Administration, Reviewer Guidance, Validation of Chromatographic Methods, FDA, Rockville, MD, Nov 1994.